

## Sediment dynamics in the subaquatic channel of the Rhone delta (Lake Geneva, France/Switzerland)

J. P. Corella · A. Arantegui · J. L. Loizeau ·  
T. DelSontro · N. le Dantec · N. Stark ·  
F. S. Anselmetti · S. Girardclos

Received: 17 December 2012 / Accepted: 11 September 2013 / Published online: 5 October 2013  
© Springer Basel 2013

**Abstract** With its smaller size, well-known boundary conditions, and the availability of detailed bathymetric data, Lake Geneva's subaquatic canyon in the Rhone Delta is an excellent analogue to understand sedimentary processes in deep-water submarine channels. A multidisciplinary research effort was undertaken to unravel the sediment dynamics in the active canyon. This approach included innovative coring using the Russian MIR submersibles, in situ geotechnical tests, and geophysical, sedimentological, geochemical and radiometric analysis techniques. The canyon floor/levee complex is characterized by a classic turbiditic system with frequent spillover events. Sedimentary evolution in the active canyon is

controlled by a complex interplay between erosion and sedimentation processes. In situ profiling of sediment strength in the upper layer was tested using a dynamic penetrometer and suggests that erosion is the governing mechanism in the proximal canyon floor while sedimentation dominates in the levee structure. Sedimentation rates progressively decrease down-channel along the levee structure, with accumulation exceeding 2.6 cm/year in the proximal levee. A decrease in the frequency of turbidites upwards along the canyon wall suggests a progressive confinement of the flow through time. The multi-proxy methodology has also enabled a qualitative slope-stability assessment in the levee structure. The rapid sediment loading, slope undercutting and over-steepening, and increased pore pressure due to high methane concentrations hint at a potential instability of the proximal levees. Furthermore, discrete sandy intervals show very high methane concentrations and low shear strength and thus could correspond to potentially weak layers prone to scarp failures.

---

This article is part of the special issue “éLEMO – investigations using MIR submersibles in Lake Geneva”.

**Electronic supplementary material** The online version of this article (doi:10.1007/s00027-013-0309-4) contains supplementary material, which is available to authorized users.

---

J. P. Corella (✉) · S. Girardclos  
Department of Earth Sciences, Environmental Sciences Institute (ISE), University of Geneva, 13 Rue des Maraichers, 1205 Geneve, Switzerland  
e-mail: pablo.corella@mncn.csic.es

*Present Address:*

J. P. Corella  
Museo Nacional de Ciencias Naturales (MNCN/CSIC), Serrano 115bis, 28006 Madrid, Spain

A. Arantegui  
Department of Earth Sciences, University of Zaragoza, c/Pedro Cerbuna, 12, 50009 Zaragoza, Spain

J. L. Loizeau  
Institut F.-A.-Forel, University of Geneva, 10 route de Suisse, 1290 Versoix, Switzerland

T. DelSontro · F. S. Anselmetti  
Eawag (Swiss Federal Institute of Aquatic Science and Technology), 133 Überlandstrasse, 8600 Dübendorf, Switzerland

N. le Dantec  
Ecological Engineering Laboratory (ECOL), Swiss Federal Institute of Technology (EPFL), 1015 Lausanne, Switzerland

*Present Address:*

N. le Dantec  
CETMEF, Technopôle Brest Iroise, 155 Rue Pierre Bouguer, 29280 Plouzané, France

N. Stark  
MARUM, Centre for Marine and Environmental Sciences, University of Bremen, Leobener Str, 48359 Bremen, Germany

**Keywords** Subaquatic channel · Sedimentary processes · Rhone delta · Levee architecture

## Introduction

Subaquatic canyons in river deltas are major pathways for transport of terrigenous detritus from land to deep-water basins in both lacustrine and marine systems. They constitute very dynamic environments affected by several sedimentological processes controlling the thalweg incision and overbank deposition. In the long term, hydroclimatic patterns and water-level changes govern the interplay between sediment supply and accommodation space. On shorter time scales, the pace of sediment supply is affected by the periodicity and magnitude of phenomena like subaquatic landslides and river floods, which generate fluctuations in the transfer of sediment through underwater channel systems. Anthropogenic factors also contribute to these fluctuations and comprise modifications of sediment discharge by dams for hydro-electricity (Anselmetti et al. 2007; Finger et al. 2006), dredging for granular materials and river channel alterations. Sediment properties such as cohesion, which are often inherited from the long-term history of sedimentation, influence the mechanisms causing short-term fluctuations in sediment supply, like landslides (Edmonds and Slingerland 2010). Scarp failures are one of the key factors controlling the changing morphology and sediment budget in subaquatic channels (Sturm and Matter 1978; Siegenthaler and Sturm 1991; Girardclos et al. 2007). They are a potential source for strong down-channel gravity flows and can be triggered by numerous processes such as rapid sediment loading, earthquakes, storm driven waves and currents, gas expulsion or slope undercutting (Hampton et al. 1996; Locat and Lee 2002; Girardclos et al. 2007; Strasser et al. 2007). Identification of subaquatic landslide triggers is a challenge for geologists and constitutes a crucial goal to prevent tsunami-related hazards and damage to deep-water and coastal infrastructures (e.g., Driscoll et al. 2000; Kremer et al. 2012).

Dynamic processes governing sediment supply significantly alter the deltaic environment. Evaluating the

relative importance of these processes is central to the elaboration of precise reconstructions or predictions of the evolution of subaquatic channels in the marine realm (Migeon et al. 2006). Besides the classic seismic reflection and core-based studies, recent advances in multibeam bathymetric systems opened new ways of precisely quantifying erosional and depositional fluxes in deep-water submarine channels (Smith et al. 2005, 2007; Noda et al. 2008; Mountjoy et al. 2009; Yoshikawa and Nemoto 2010; Conway et al. 2012; Hughes Clarke et al. 2012). However, more efforts and new techniques are needed in particular to understand remobilization processes in subaquatic environments. Small-scale dynamic penetrometers are reliable tools to test in situ geotechnical behavior of underwater sediments and to complement the investigation of subaqueous sediment dynamics (Stark et al. 2009a, 2011; Stark and Kopf 2011).

Lake Geneva (Switzerland/France) is the largest fresh-water lake in Western Europe (Fig. 1). The lake is located in the Alpine foreland basin between the Jura Mountains and the Alps and was carved by glacial incision during the Pleistocene (Wildi and Pugin 1998). The Rhone River runs from the Alps through Lake Geneva to the Mediterranean Sea. The mean annual discharge of the Rhone River for the period 1935–2008 ranged between 127 and 227 m<sup>3</sup>/s at the “Porte-du-Scex” gauging station, located 6 km upstream of the river mouth (OFEV 2009). The annual sediment load transported by the Rhone river into Lake Geneva varies between 2 and 9 × 10<sup>6</sup> t/year (Burrus et al. 1989) and provides the supply for the large delta located in the eastern part of the lake. The detailed underwater morphology of the Rhone delta, revealed by a recent high-resolution bathymetry survey, shows significant depositional and erosional processes along the submarine canyons (Sastre et al. 2010). The modern active canyon of the Rhone River is a 14 km-long sinuous subaquatic channel (Fig. 1). It is characterized by a complex canyon-levee system (Houbolt and Jonker 1968; Giovanoli 1990). The northeastern levee is higher than the southwestern levee, likely due to water circulation at the delta. The Coriolis effect causes current flow to be predominantly northward, which in turn induces differentiated sedimentation on the northeastern and southwestern sides of the channel (Loizeau 1991). Channel relief (i.e. elevation difference between the levee crest and the channel floor) ranges from over 50 m in proximal areas to below 20 m in distal areas (Fig. 1). The canyon floor, or “axial canyon”, is characterized by widespread undulating sandwaves in the proximal and central areas (0.5–2 m height; 30–100 m width), suggesting current velocities of 0.5–1 m/s (Girardclos et al. 2012). Consistently, Lambert and Giovanoli (1988) demonstrated the existence of density currents formed by river underflows plunging below the lake surface and mass-movement processes triggered

### Present Address:

N. Stark  
Department of Civil and Environmental Engineering,  
Virginia Tech, Patton Hall, Blacksburg, VA 24061, USA

### Present Address:

F. S. Anselmetti  
Institute of Geological Sciences, Oeschger Centre for Climate  
Change Research, University of Bern, 1-3 Baltzerstrasse,  
3012 Bern, Switzerland

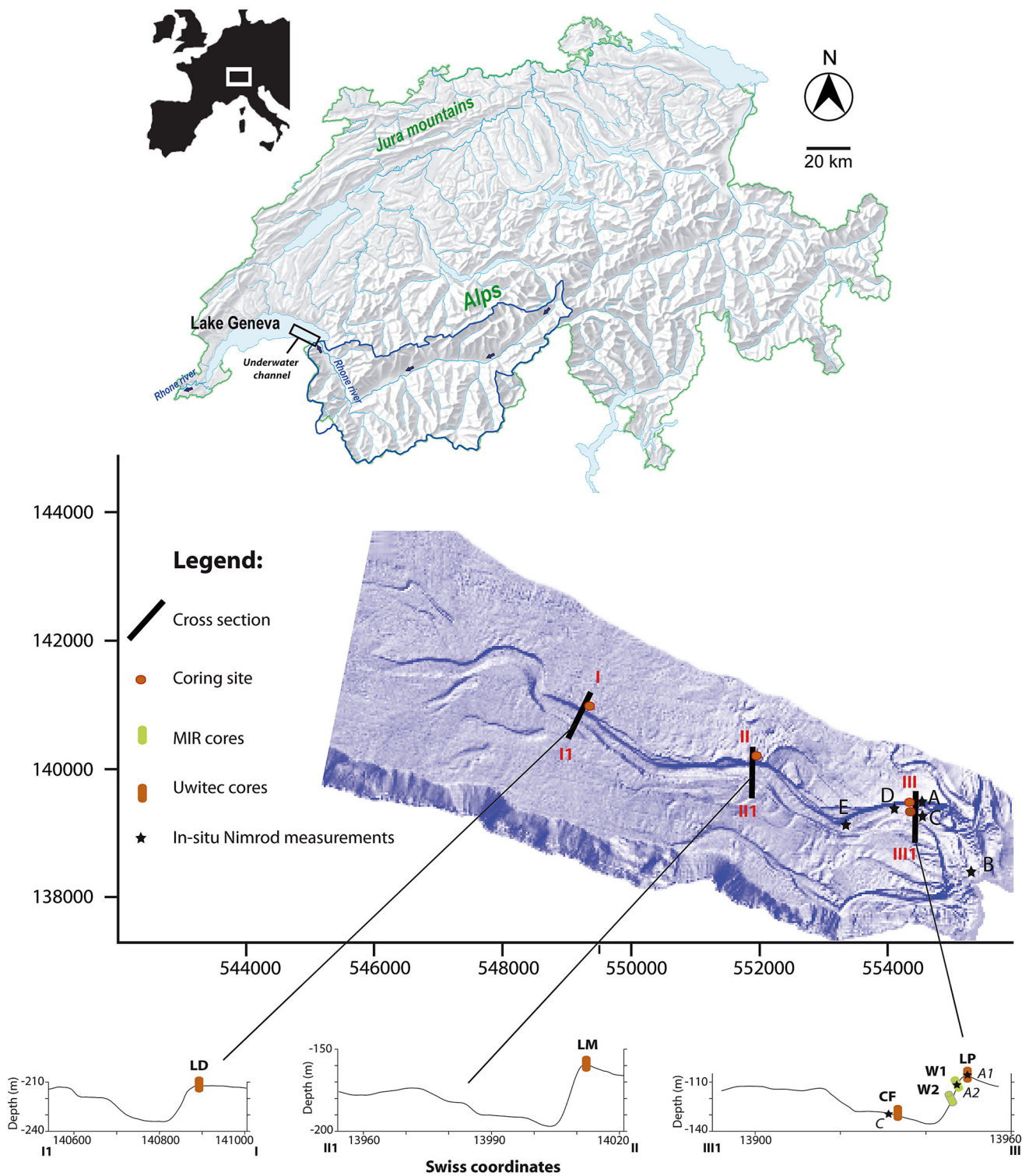


**Fig. 1** Top Location of study area and shaded relief map of western Switzerland. Rhone River catchment is indicated with blue lines. High-resolution multibeam bathymetric map from 2008 (swiss coordinates—number of swiss grid are given in meters)—Data

courtesy of Institut F.-A. Forel, University of Geneva published in Sastre et al. (2010). Bottom bathymetric profiles, location of retrieved cores and in situ Nimrod measurements are indicated by asterisks (color figure online)

by frequent scarp failures in the active canyon. Meybeck et al. (1991) presented chemical evidence of surface water intrusion in the deepest parts of Lake Geneva. No such

sandwaves were found in distal areas, probably reflecting a decrease in the velocity of the flow downslope along the axis of the canyon (Girardelos et al. 2012).

Since the pioneer work of Forel (1885), the subaquatic channel of the Rhone delta is historically referred to as an example of the erosive power of sediment-laden currents (Houbolt and Jonker 1968; Shepard 1979; Giovanoli 1990), although there are only limited in situ measurements available (Lambert and Giovanoli 1988), and erosion rates have only been partly quantified (Loizeau 1991). The objectives of this study were: (i) to reveal new insights into the complex erosion and sedimentation processes in the main sublacustrine canyon by combining innovative coring, sedimentological analyses and geotechnical methods; (ii) to provide an age model of the levee sequences based on radiometric techniques; and (iii) to qualitatively assess slope stability of the canyon walls. Ultimately, this research is relevant to the understanding of the levee architecture and channel-levee morphology and its relation to sediment dynamics in deep water channels.

## Materials and methods

Four *Uwitec* gravity sediment-cores were retrieved in August 2011 from the proximal canyon floor (CF, 130 m depth) and from proximal (LP), middle (LM) and distal (LD) areas in the northern levee (LP, 103 m water depth; LM, 160 m water depth; LD, 220 m water depth; Fig. 1). Standard gravity coring does not allow retrieval of sediment cores from the inclined canyon walls. Thus, an innovative coring method, fully explained in Girardclos et al. (2012), was applied using the MIR submersibles operated by the Russian Academy of Sciences. Two sediment cores W1 and W2 were collected in the northern canyon wall (W1, 112 m water depth; W2, 120 m water depth) at 9 and 17 m sediment depth below levee top (LP), respectively. All cores were split lengthwise in two halves and pictures were taken using a digital camera under controlled light conditions. Sediment lithology was visually described including colour, textures and grain-size distribution. Physical properties were measured every 5 mm with a Geotek multi-sensor core logger (MSCL) at the ETH Zurich Limnogeology Laboratory. Grain-size distribution was measured every 1–2 cm with a Mastersizer 2000 particle-size analyzer at the Pyrenean Institute of Ecology (Zaragoza, Spain). Samples were pre-treated by adding 10 ml of dispersant (sodium polyphosphate) to the solution. Grain-size data was processed using GRADISTAT software (Blott and Pye 2001). All cores retrieved in the levee were sampled every 1–2 cm for total carbon (TC) and total nitrogen (TN) using an elemental analyser (Hekatech Euro EA, Germany) and for total inorganic carbon (TIC) using titration coulometry (Coulomat 5015 CO<sub>2</sub>-Coulometer, Coulometric Inc., USA) at Eawag (Switzerland). Total organic carbon (TOC) was calculated as difference between TC and TIC. AMS

radiocarbon dating on microcharcoal particles, obtained by sieving one entire half of the split sediment core, was carried out at ETH Zurich (Switzerland). Radiocarbon dates were calibrated using the INTCAL 09 calibration curve (Reimer et al. 2009) and the OxCal 4.1 software. The recent sediment on the levee top was dated by gamma spectrometry using the <sup>137</sup>Cs activity method on dry sediment with HPGe well-type detectors (Ortec, GWL series, USA) at the Institute Forel (University of Geneva, Switzerland).

In situ geotechnical tests were performed using the small-scale dynamic penetrometer NIMROD, developed for rapid geotechnical characterization of the upper-most sediment surface of the lake/sea floor (Stark et al. 2012). Dynamic penetrometers allow quantification of sediment mobilization and accumulation processes by evaluating the sediment strength along a vertical profile and identifying layering in the strength of shallow sediments deposits (Stark et al. 2011). NIMROD measurements were carried out from a small research vessel in the proximal canyon floor, canyon wall and top levee (Fig. 1). The impact velocities along this transect were homogeneous ( $\approx 2$  m/s), and the penetration depth ranged between 6 and 26 cm. The approach introduced by Stark et al. (2009b) was used to estimate an equivalent of quasi-static bearing capacity (QSBC) that accounts for changes in penetration velocity, which result in non-linear coupling effects between the measured deceleration and an estimate of sediment strength. Here, QSBC was determined for a constant penetration velocity of 2 cm/s and the NIMROD with conical tip geometry (Stark et al. 2009b). Complementary shear-vane tests were carried out on the open sediment cores at a 5 cm spacing using a HM-504A pocket shear-vane device, with a rotation speed of  $\sim 30$ – $40^\circ$ /min until the peak shear strength was exceeded. The first 5 cm were not tested due to the water loss and consolidation of the sediment during storage.

To measure methane in the sediment porewater, a core was taken using a liner with holes drilled every centimeter and covered with tape for deployment. Immediately after retrieving the core, a cut-off syringe was used to extract 2 ml of sediment, which was preserved in 25 ml serum bottles containing 4 ml of NaOH. Methane was measured using gas chromatography and a flame ion detector (Agilent 6890N Network Gas Chromatograph) and concentration was calculated using Henry's Law. See Sollberger et al. (2013) for more sampling details.

## Results

### Lithology in the Rhone delta canyon

The subaquatic canyon system of the Rhone delta exhibits the classic alternating hemipelagic and turbiditic



sedimentation punctuated by frequent debris-flow deposits in distal areas (Lambert and Giovanoli 1988). In the proximal canyon floor, turbidites are recognized as to dm- to cm-thick fine-to-coarse sand layers with a fining upward texture topped by a layer of finer sediments (mean grain size = 56  $\mu\text{m}$ , Fig. 2b, c). These turbidites show a basal sub-layer of coarser, relatively well-sorted material (mean grain size = 208.5  $\mu\text{m}$ ). The top fine-grained layers are frequently absent in proximal areas (core CF; Fig. 2b, c).

The northern levee displays sub-horizontal strata of alternating hemipelagic and turbidite facies (Figs. 2 and 3). Hemipelagic sediments (mean grain size = 36.6  $\mu\text{m}$ ) consist of laminated mm-thick light grey to brownish silty layers and white laminae that represents the background sedimentation of the lake. This facies are also characteristic of former inactive canyons in the eastern area of the delta (Wunderlin et al. 2013). In the active canyon, hemipelagic facies are intercalated by mm- to cm-thick layers of detrital origin that represent the allochthonous input into the lake, mostly transported within the river plume and dispersed as interflow. Turbidites in the levees are poorly sorted and fine skewed, showing a grain-size decrease from proximal to distal areas (Fig. 4). A comparison of the cores retrieved in the wall and the top surface along the same canyon transect in the proximal levee (Fig. 2) reveals that frequent turbidites occur in core W2 (taken in the canyon wall, 17 m lower than the top surface of the levee). On the other hand, relatively scarce turbiditic layers appear in top levee sediments (LP core).

In regard to the geochemical composition of the sedimentary record, TOC and TIC profiles are relatively homogeneous in the studied cores, showing low values in both proximal and distal levees (0–3 %). The high C/N ratio in the levee sediments, with mean values between 14.5 and 22.4, highlights the terrestrial origin of the organic matter (Meyers 2003; Fig. 1 in the supplementary material).

#### Geotechnical testing

In-situ geotechnical surveys were performed in a proximal transect across the levee and along the canyon floor (Fig. 1; Table 2) to provide complementary information of the ongoing sediment dynamics in this area as a snapshot in space and time. Measurements A1, A2 and C were carried out in the proximal transect close to the coring sites (cores LP, W1 and CF, Figs. 1 and 2) reaching penetration depths from 6 to 26 cm. The lowest sediment strengths were found on the top levee (site A1 and A2; QSBC =  $2.4 \pm 0.5$  and  $3.4 \pm 0.4$  kPa, respectively), while the highest QSBC equivalents were observed in the axial channel (site C; QSBC =  $24 \pm 4$  kPa) (Table 2). The lower sediment

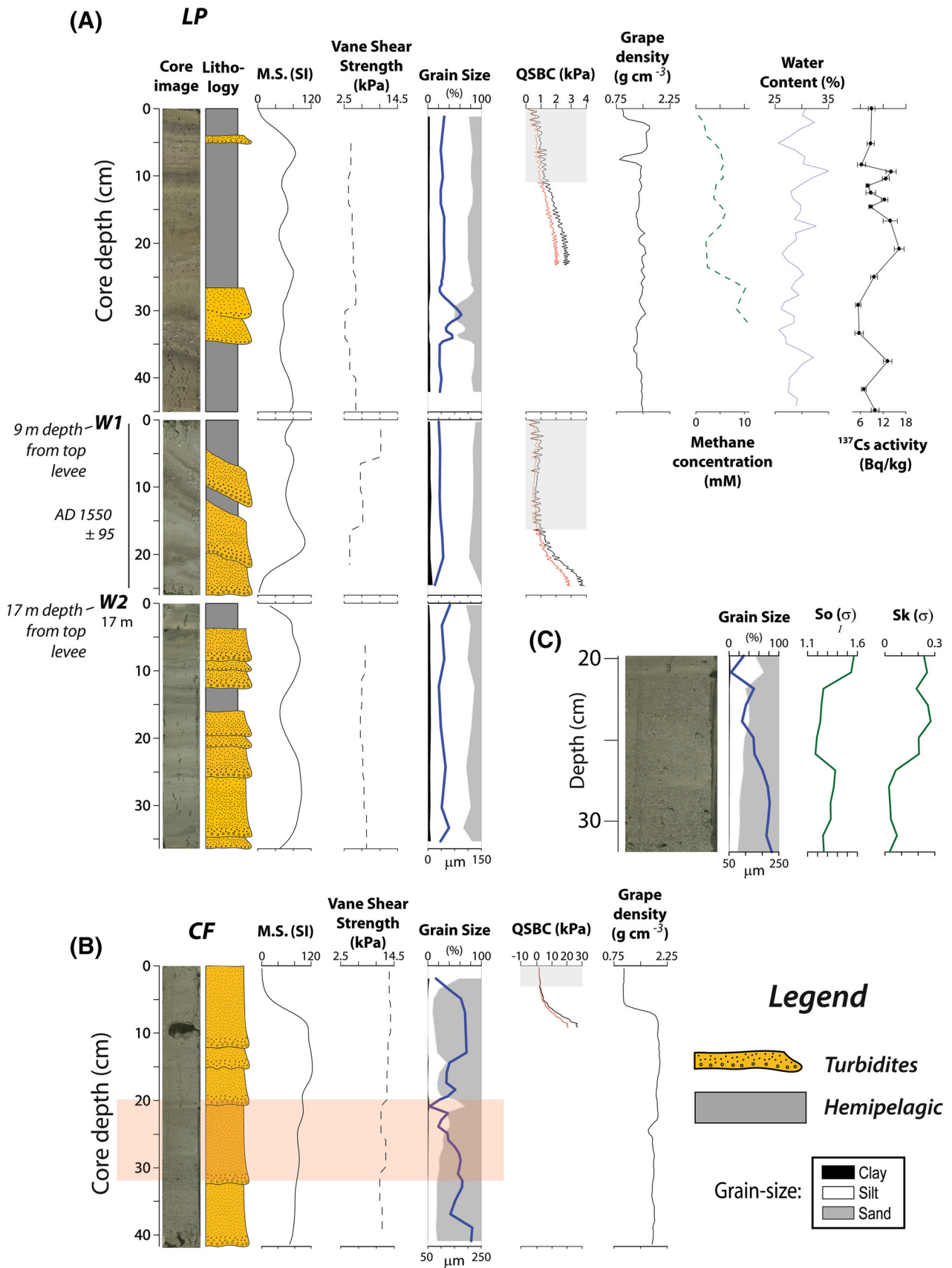
strength in the top levee compared to the canyon wall located 9 m deeper is attributed to a 30 % increase in sediment compaction along the levee structure. This percentage is in agreement with the estimated 20–40 % water loss in the upper 9 m of the levee sediments reported in Girardclos et al. (2012).

Additional measurements B, D and E were made along the canyon floor (18, 145, 167 m water depths, respectively, Table 2). Proximal sites B ( $\approx 100$  m from the river mouth) and C showed the largest QSBC equivalents ( $24 \pm 0.6$  and  $24 \pm 4$  kPa). A thin top-layer thickness of soft sediment (2–3 cm) in the axial channel corresponds well with the soft top-layer thickness in the levee (LP and W1 cores). The top layer progressively thickens up to 8 cm towards distal site E (167 m depth,  $\approx 3$  km from the river mouth), where low QSBC and excess pore pressure indicate a soft lake floor (Table 2).

Vane-shear tests show an increase in mean shear strength from 4.1 to 5.4 kPa in cores LP and W1 (Fig. 2), which is consistent with QSBC estimates obtained using the NIMROD. The difference between both methods are attributed to the different measuring procedures (in situ versus laboratory testing, e.g., drainage of cores, loss of original sediment texture during transport and storage) and in data presentation between dynamic penetrometer and vane shear results (e.g., Stark et al. 2009b, 2012). Down-core, vane-shear tests indicate reduced shear strength on the coarser basal sub-layer of thick turbidites (Figs. 2 and 4), suggesting that sandy material constitutes weak, poorly consolidated layers.

#### Sedimentation rate of the levee

$^{137}\text{Cs}$  activity in cores LP, LM and LD was generally low (6–26 Bq/kg, Figs. 2 and 3). Assuming no downward migration of  $^{137}\text{Cs}$  and/or reworking processes (Dominik et al. 1992), this radiometric dating suggests that deposition postdates AD 1954, and enables us to calculate minimum sedimentation rates (SR) of 0.79 cm/year in LP, 1.16 cm/year in LM, and 0.68 cm/year in LD. An ill-defined peak (26 Bq/kg, Fig. 3) occurs at 48–49 cm in core LM that may correspond to the 1986 Chernobyl accident. According to this peak, mean sedimentation accumulation rate in core LM ( $\approx 4$  km from the river mouth) is 1.9 cm/year. Two radiocarbon dates were obtained from sediment cores W1 and W2 in the proximal canyon floor (9 and 17 m sediment depth from the top levee, respectively, Figs. 1 and 2). The radiocarbon date from W2 core (120 m deep) (Table 1) was not considered due to contamination of the liner of core W2 during a previous coring operation at site W1, 9 m deep from the top levee. The calibrated  $^{14}\text{C}$  date from W1 core (113 m water depth, 9 m sediment depth from the top levee) yielded a SR of  $2 \pm 0.4$  cm/year for



◀ **Fig. 2** Sediment cores retrieved in the top levee and canyon wall of the northern levee (a) and canyon floor (b) of a proximal canyon transect (Fig. 1). From left to right (a and b): Depth below the levee top (m); core depth (cm); Sediment-core images, lithology, magnetic susceptibility ( $\times 10^{-5}$ ), vane-shear strength, grain-size (blue line indicates the mean grain-size), QSBC-depth profile (constant penetration velocity of 0.02 m/s, red and dark lines indicate maximum and minimum values showing the range resulting from empirical factors used for estimating QSBC (Stark et al. 2009b), the grey band indicate the thickness of the soft top-layer (Table 2)), Grape (gamma-ray attenuation porosity evaluator) density, methane concentration (Sollberger et al. 2013), water content and  $^{137}\text{Cs}$  activity profile. Radiocarbon date in core W1 is also indicated. (C): Detail of the thick turbidite in CF sediment core (20–33 cm depth) and grain-size profile and distribution parameters (0.5 mm resolution, *So* Sorting, *Sk* Skewness) (color figure online)

the upper 9 m of the sedimentary sequence, which is significantly higher than the SR in middle and distal areas of the active canyon. Considering the compaction of the sediment in the upper 9 m of the sequence and assuming a constant SR during the last 400–500 years, recent surface sediments would have been accumulating at a 30 % higher rate (2.6 cm/year).

#### Methane

Methane was measured in LP and LD every 1 cm for 10 cm then every 2 cm until the bottom of the core. The first 10 cm in proximal core LP showed a typical increasing profile with concentrations stabilizing more or less around 5 mM at 20 cm depth (Fig. 2). A slight decrease in concentrations occurred between 20 and 26 cm depth followed by a sudden increase to 10 mM, at the same level as the large turbidite at 26 cm (Fig. 4). Lower values occur in distal core LD, with a constant profile displaying values of 1 mM down to the turbidite at 15 cm, where another abrupt increase to 9 mM occurs. Concentrations remained high within the turbidite layer in both proximal and distal cores (Fig. 4).

#### Discussion

##### Sedimentological processes in the Rhone delta canyon

Density currents strongly modulate the geometry and sedimentation of the Rhone sublacustrine channel. These processes are a result of underflow events due to hyperpycnal currents and/or mass-movement processes, a common feature in the sediment dynamic of active canyons (Inman et al. 1976; Sturm and Matter 1978; Xu et al. 2004; Canals et al. 2009; Mulder et al. 2012). The texture of the turbidite deposits in the studied channel, particularly the presence of a thin basal sub-layer of coarser material, indicates that most turbidites are flood-related sediments deposited at the canyon floor (Mulder and Alexander 2001;

Wirth et al. 2011; Corella et al. 2011). The grain-size distribution parameters of the turbidites in the canyon floor are in agreement with high turbulence events modelled by Baas et al. (2005) in laboratory experiments. The near symmetrical to positive skewness evolution from bottom to top of the turbidite shown in Fig. 2c suggests the upper limit to the grain size that the hyperpycnal currents can transport as bedload.

The likely erosion of the top fine-grained layer in the proximal canyon floor (Fig. 2) suggests ongoing erosional processes in this area produced by density currents that occur in the axial channel. A comparative approach combining geotechnical and sedimentological analyses reveals higher sediment strength and density values, more intense erosion of turbidite layers and lower top-layer thickness in the canyon floor (Fig. 2; Table 2) compared to the northern levee. In addition, the better sorting of the sediment in the canyon floor in comparison with the levee indicates that finer particles are washed out in the axial channel (Fig. 4c). Such observations on the mechanical properties and stratigraphy of sediments hint at ongoing transport and recent erosion of surface sediments in the canyon floor. The eroded surface in the canyon floor is harder and more compacted than the northern levee where sedimentation dominates with accumulation rates of 2.6 cm/year. As turbidites move down canyon, they transfer mobilized sediment from the through-channel flow to the levees as an overspilling turbulent flow, depositing poorly sorted turbidites in the levees (Fig. 4c). In areas of sediment remobilization and deposition, a soft, loosened-up top layer, as detected in the vertical geotechnical profiles, probably represents stirred up sediment in the process of sediment remobilization, or sediment recently deposited with a lower state of consolidation (Stark and Kopf 2011; Stark et al. 2011). Thus, a thick top layer on the levee, where current velocities are expected to be lower than on the thalweg, i.e. the main pathway of turbidites, is likely related to deposition of suspended sediment that was spilled over the major transport path.

The inferred erosional processes in the proximal canyon floor are in agreement with a recent study in the area (Girardclos et al. 2012) highlighting predominant erosion in proximal areas of the canyon floor. Two comparative multibeam surveys carried out in 2008 and 2012 (Girardclos et al. 2012) reveal a total vertical erosion of 2 meters in the canyon floor section between sites B and C (18–130 m depth). These erosional patterns indicate the erosive power of sediment-laden hyperpycnal currents, which have been observed to reach velocities of up to 0.9 m/s in this subaquatic channel (Lambert and Giovanoli 1988).

The decrease in the frequency of turbidites in the proximal levee (Fig. 2) reflects the erosion vs. deposition

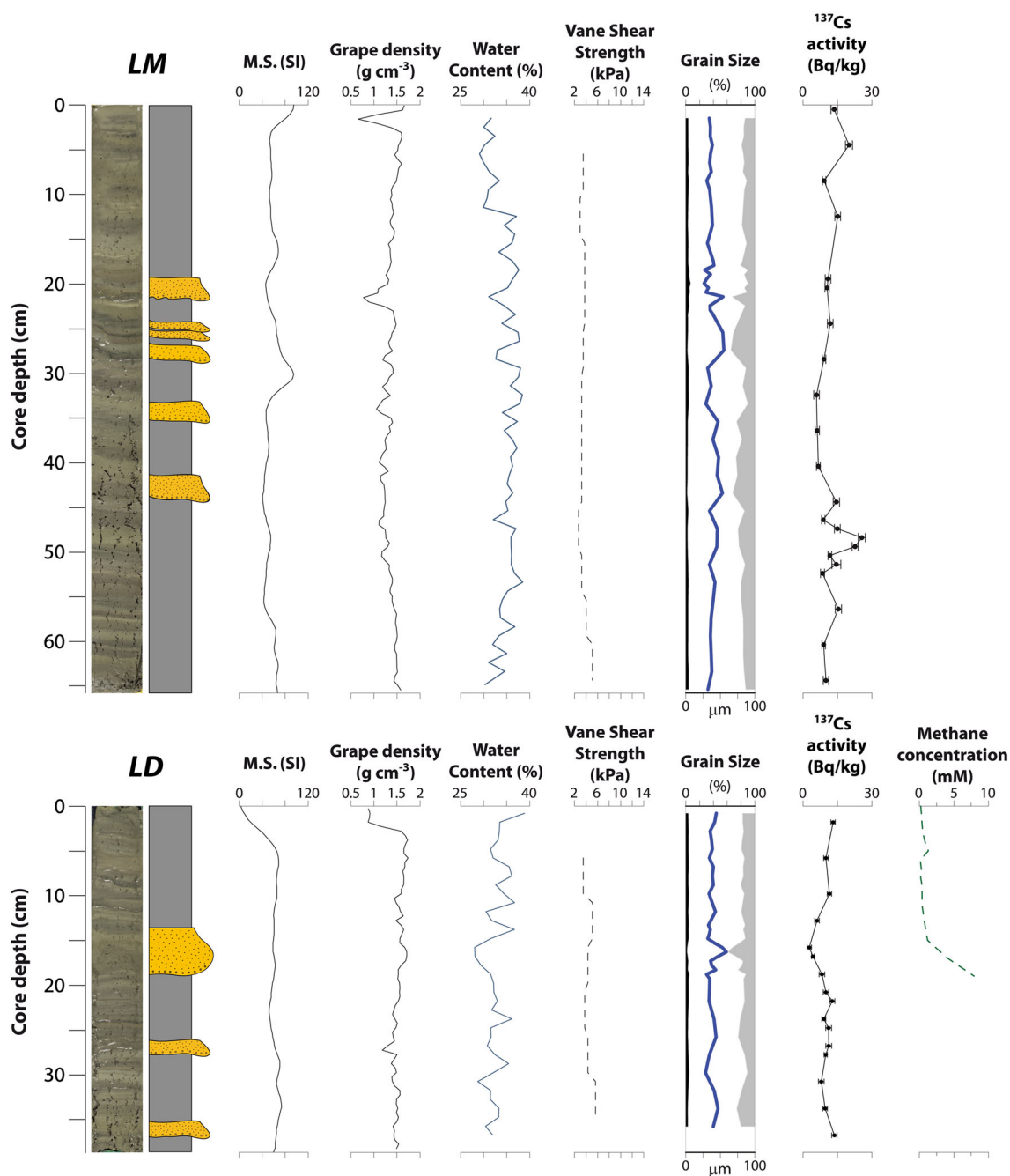


**Fig. 3** Sediment cores retrieved from the levee top from middle (*LM*) and distal areas (*LD*). From *left to right*: Core depth (cm), Sediment-core images, lithology, magnetic susceptibility ( $\times 10^{-5}$ ), Grape density, water content, vane shear strength, grain-size (*blue line*

indicates mean grain-size), XRF data, TIC, TOC and C/N ratio,  $^{137}\text{Cs}$  activity profiles and methane concentration (Sollberger et al. 2013). Legend is shown in Fig. 2 (color figure online)

behavior mentioned above. Continuous deposition on the levee and erosion along the axial channel intensified the channel relief and makes the overbank flow of subsequent turbidity currents less likely (Houbolt and Jonker 1968). Therefore, only extreme events leading to thick sediment-laden currents can currently generate an overspill of material in proximal areas depositing material outside the

canyon. The 9 cm-thick turbidite in the top sediments of the proximal levee (core LP; 35–26 cm depth) reinforces this hypothesis as it was most likely deposited during an extreme event: the exceptional October 2000 AD flood, which reached almost  $1,400 \text{ m}^3 \text{ s}^{-1}$  close to the lake inlet and displays a return period of  $>300$  years (OFEV 2009; Fig. 4b). This turbidite event reached middle and distal



**Fig. 4** **a** Main features of the 2000 AD turbidite shown in cores LP, LM and LD (*methane bubbles* are indicated with *red circles*). **b** (Left) Rhone river water discharge evolution during October 2000 AD measured at Porte du Scex hydrological station. (Right) Historical floods record of the Rhone river, displaying the highest annual peaks in water discharge at Porte du Scex hydrological station for the period 1905–2010 (Data courtesy of the Office Fédéral de l'Environnement and published in OFEV 2009). **c** Ternary plot and skewness vs. sorting diagram showing turbidite grain-size parameters from CF, LP, LM and LD cores (color figure online)

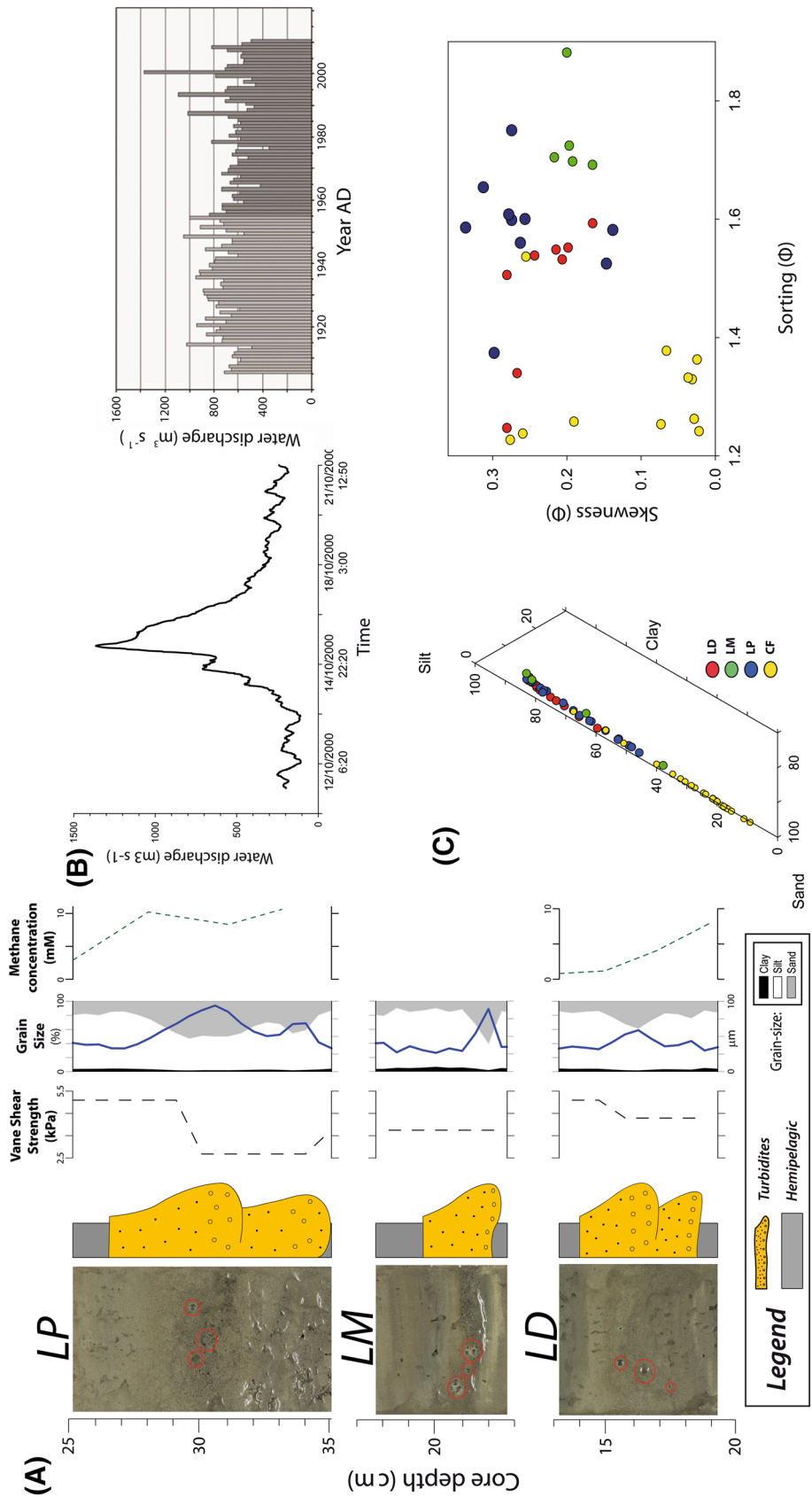


**Table 1** Radiocarbon dates obtained in the Rhone delta (Lake Geneva) proximal levee in W1 and W2 sediment cores

	Core depth (m)	Lab code	Material	<sup>14</sup> C year BP	Calibrated years AD (10 range 68.2 %)
	W1 (9 m)	ETH-44253	Charcoal, plant remains	315 ± 45	1,585 ± 65
Age labeled with an asterisk was rejected (see text)	W2 (17 m)*	ETH-44252	Charcoal, plant remains	320 ± 30	1,555 ± 45

**Table 2** Geotechnical results from in situ Nimrod tests in sites shown in Fig. 1

Site	Penetration depth (cm)	Impact velocity (m/s)	Deceleration (g)	QSBC (kPa)	Top layer thickness (cm)	Hydrostatic pressure (kPa)	Excess pore pressure (kPa)
A1	26	2	2	2.4 ± 0.4	11	949	13
A2	26	2	3	3.4 ± 0.5	16	1,255	10
B	6	3	12	24 ± 0.6	2	1,300	28
C	6	2	12	24 ± 4	3	1,233	43
D	7	2	10	17.5 ± 2.5	5	1,394	33
E	21	2	1	1.6 ± 0.3	8	1,412	2

The shown deceleration and QSBC represent the maxima reached during the respective deployments

areas of the levee and reflects the two different pulses of the flood that occurred on 14 and 15 October with water discharge of 1,090 and 1,360 m<sup>3</sup> s<sup>-1</sup>, respectively (Fig. 4a, b). Nevertheless, another exceptional event such as the large mass movement that occurred in the active canyon in 2000 AD, involving 5 × 10<sup>6</sup> m<sup>3</sup> of sediment transported from proximal to distal areas of the channel (Sastre 2003), might also be the triggering mechanism for the turbidite deposit shown in Fig. 4. Thus, through-channel flow characteristics and levee architecture are closely related. The evolution of the proximal channel-levee complex over time, with increasing confinement of the underflows into the sublacustrine channel and decreasing frequency of overbank deposits, occurring only during exceptional events, as indicated in the core data, was previously hypothesized by Komar (1973).

The increase of fine material down-channel (sites LM and LD) is indicative of a decrease in flow velocity. Flow deceleration towards distal areas is further supported by the increase in top layer thickness from sites B to D (18–167 m depth; Table 2), interpreted as settling of suspended matter and reduced remobilization processes as the flood current decelerates down-channel. Sediment bedforms observed in and around the canyon confirm the flow deceleration hypothesis for common, low-intensity turbidite events (Houbolt and Jonker 1968). The sudden disappearance of undulating sand dunes from the axial channel between 225 and 260 m water depth and their presence outside the channel at those depths (Girardclos et al. 2012) could be explained by a progressive down-channel loss on flow confinement associated with flow deceleration. A likely change in the hydrodynamic conditions caused by slope angle decrease at 200–250 m depth could likely trigger a

flow stratification, extinguishing the turbulence near the bed and thus avoiding the re-entrainment of sediment particles into suspension and the reworking of sediment at the base of the flow, as previously demonstrated in numerical simulation of turbidite currents (Cantero et al. 2012). This lack of basal reworking would explain the lack of internal structures in the canyon floor. Girardclos et al. (2012) also proposed a possible flow deceleration at 250 m depth based on an abrupt change in surface morphology of the medium-scale sediment structures in the axial channel. The shift from undulatory asymmetrical ripples to small linguoid ripples points to reduced flow velocities from about 0.5 to 0.25 m/s (Reineck and Singh 1986). Nevertheless, the lack of measurements on sediment concentration, velocity profiles at the base of the water column and more information about how the bedforms restructure are inconclusive and more investigation would be needed to validate these hypothesis. Visual observations during MIR dives in the axial channel also enable the identification of a detachment of the underflow at 250 m depth where the head of the hyperpycnal inflow was progressively dissipating and migrating upwards (Richard Camilli, pers. comm.). The detachment results from both a progressive decrease of the density gradient between river inflow and lake water and a decrease in flow velocity. This process causes an increase in flow thickness and the development of a spreading flow towards distal areas as suggested by Skene et al. (2002) in other deep-water levee records.

The canyon floor and levees are both directly experiencing the spreading flow and subsequent sediment transport, in contrast with the overspilling flow type in proximal areas where the channel is the main conduit for the transport of sediment to the distal fan. Sedimentation

on the levees results mostly from deposition of materials transported in the axial channel and normal hemipelagic sedimentation. Observed grain-size variability is likely related to the two flow regimes, evolving from well-defined coarse sandy turbidites within a silty background in proximal areas, where overspilling dominates (core LP), to a progressive change to the deposition of sediment with a more uniform grain-size distribution (Core LD), related to the spreading flow. This generic pattern is very well seen in the Hueneme Fan (Normark et al. 1998) and fully discussed in Skene et al. (2002). The sedimentation rates obtained in proximal and distal levees in the Rhone delta channel (LP, 2.6 cm/year; LM, 1.9 cm/year; LD, >0.78 cm/year) are consistent with the age model proposed by Giovanoli (1990) and Loizeau (1991) and for recent sediments by Loizeau et al. (2012). Radiometric data show a progressive decrease in sedimentation rate with the distance from the river mouth certainly due to the progressive loss of suspended material down channel. A down-channel decreasing sedimentation rate is in agreement with physical laboratory experiments (Kane et al. 2010) and with observations in other levee sequences around the world—e.g., Northwestern Atlantic Mid-Ocean Channel and Reserve and Van fans (see summary in Skene et al. 2002).

#### Forcing mechanisms controlling sediment dynamics in the canyon

External factors controlling downslope flows drive the sedimentary dynamics on subaquatic sediment conduits. Underflow processes due to hyperpycnal currents are related to flood frequency and magnitude, so that turbidite frequency also should vary with lake level and climate change (Mulder et al. 2003). In addition to sediment supply variability corresponding to natural processes operating on long time scales, the Rhone delta provides wide evidence of the impact of human activities in controlling the sediment budget and processes in Lake Geneva. Loizeau and Dominik (2000) showed that the hydraulic management of the lake since 1883 and the building of hydroelectric reservoirs in the upstream Rhone river watershed have significantly altered the natural flow characteristics and the sediment dynamics in the active canyon during the last century. Loizeau and Dominik (2000) also highlight that sediment input to the lake has been reduced by a factor of two and the eroding power of the hyperpycnal currents has diminished due to the reduction of large floods.

Internal lake processes also contribute to sediment dynamics in the canyon and delta, in particular to turbidite generation (Lambert and Giovanoli 1988; Meybeck et al. 1991). Houbolt and Jonker (1968) and Sastre (2003) showed that turbidites, interpreted as underflow deposits, remain frequent in the lake record after the construction of

upstream reservoirs. Hydrological data show that the number of large floods drastically diminished after dam construction (Loizeau and Dominik 2000), except for a large flood in 2000 AD (OFEV 2009) that probably deposited the thick turbidite observed in the levee cores LP, LM and LD (26, 19 and 14 cm depth, respectively). Thus, flood events alone cannot fully explain the recent turbidite record and the strong channel-floor erosion in recent years (Girardclos et al. 2012). Sastre (2003) suggests scarp failures as a possible key trigger of sediment-laden density currents as also described in Lake Lucerne (Siegenthaler and Sturm 1991) and Lake Brienz (Girardclos et al. 2007), with a major mass movement in 2000 AD that might also be responsible for the turbidite deposit shown in Fig. 4. The role of mass-wasting processes related to gravitational collapses must then be taken into account to explain down-canyon particle transport processes, as well as the intra-canyon sediment budget that shapes the canyon morphology. In the Rhone delta channel, records from moorings instrumented with current meters have confirmed the occurrence of density currents likely related to slope failures that could reach up to  $3 \text{ m s}^{-1}$  (Lambert and Giovanoli 1988). Recent multibeam bathymetry of the Rhone channel (Sastre et al. 2010) has revealed slide scars, particularly frequent in the proximal northern levee between 20 and 100 m depth (Fig. 1). In addition, Girardclos et al. (2012) identified new slide scars formed between 2008 and 2012 on the sidewalls of the channels, evidence slope instability currently developing in the canyon walls. Among the short-term triggers capable of generating repeated mass-movement processes on submerged lateral slopes, certain mechanisms, such as earthquake shaking and extreme floods, can be ruled out. Neither seismic nor hydrological data (except for the large 2000 AD flood) suggest those as triggering mechanisms for the numerous turbidites deposited in the Rhone delta during the last decades. Therefore, either strong underflow events occur without exceptional river inflows or other causal factors, such as sediment accumulation and oversteepening that affect slope stability over a longer time, are responsible for the development of gravitational processes.

#### Long-term factors controlling slope stability in the canyon walls

The northern levee in the subaquatic canyon of the Rhone delta is usually steeper and thus less stable than its southern counterpart as a result of the erosive imprint. Incision is most pronounced on the northern side of the channel, as can be seen in bathymetric cross-sections (Fig. 1). The multidisciplinary approach conducted in this study enables the evaluation of long-term mechanisms controlling scarp failures in the northern, unstable levee.

### *Sediment loading*

Rapid sediment accumulation in prograding deltas can cause local oversteepening and failure of recently deposited sediments (Shepard 1932; Coleman and Prior 1988; Siegenthaler and Sturm 1991; Girardclos et al. 2007). Increasing porewater pressure and sediment weight from overburden influence slope instability by increasing the shear stress downslope (Locat and Lee 2002; Sultan et al. 2004). This mechanism has been observed in other perialpine lakes in Switzerland—Lake Lucerne (Strasser et al. 2007); Lake Brienz (Girardclos et al. 2007). In the Rhone delta, very high sedimentation rates in the top levee, up to 2.6 cm/year in proximal areas, impedes the compaction of recent sediment, consistent with the reduced sediment strength that is reflected in the low values of vane-shear stress measured in cores LP, LM and LD (Figs. 2 and 3). Increasing susceptibility of slope failures with time due to progressive loading of the slopes by ongoing sedimentation in the northern levee is a likely process to explain the observed sedimentation dynamics.

### *Porewater overpressure*

Remineralization of marine or lacustrine organic matter in sediments leads to a build-up of gases in sediment porewater (Reeburgh 1983; Henrichs and Reeburgh 1987) with methane being one of the more dominant gases produced in anoxic freshwater sediments (Bastviken et al. 2004). Such biogenic methane can saturate the pore fluid and reduce inter-particle cohesion and friction, thereby reducing sediment strength (Coleman and Prior 1988; Locat and Lee 2002). In the Rhone delta, increased pore pressure is expected in the levee structure due to the high methane concentration observed in the sediments (Sollberger et al. 2013) (Figs. 2 and 3). Core LP (Fig. 2) shows higher methane concentrations compared to core LD (Fig. 3), thus also indicating unstable conditions in proximal areas. In particular, discrete sandy intervals at the base of turbidite layers display the highest methane concentrations in both proximal and distal cores, LP and LD, where abundant methane bubbles can be seen (Fig. 4). In addition, vane-shear tests suggest reduced shear strength on the coarser basal sub-layer of thick turbidites (Fig. 4). Considering possible increased pore pressure due to high methane concentration and reduced shear strength, we propose that coarser turbidites correspond to potentially weak layers that favor failure. Slide initiation would occur along failure planes developed at the lithological boundary between hemipelagic sediments and the weaker, coarser sediments of turbidite deposits. The repetitive sequence of physical and geotechnical properties along the stratigraphy of the canyon wall, caused by successive thick turbidites (Fig. 2),

ultimately controls the slope-stability equilibrium. Assessment of excess pore pressure in these weaker layers along with sediment strength would enable the identification of potential failure locations along planes at specific stratigraphic levels.

### *Subaquatic channel erosion and oversteepening*

Undercutting of the slopes by underflows increases the potential of slope failures due to oversteepening, as seen in other marine canyons, e.g. Greene et al. (2002). Deep-sea channels commonly exhibit lateral asymmetry and localization in their erosional pattern. Sastre et al. (2010) highlighted the impact of the Coriolis force-induced northward deviation of the water inflow on the morphology of the northern levees in the Rhone delta, as proposed by Loizeau (1991). In the proximal area of the Rhone delta main canyon, the combination of steep slopes (30–40°, Fig. 1) and ongoing sediment dynamics (underflow erosion in the axial channel and overspilling processes in the levees) causes a progressive increase of in channel relief that will likely increase scarp failure frequency in the future. In localized areas, such as sharp meanders, the helicoidal flow causes enhanced erosion and undercutting at the outer bend of the meanders (Peakall et al. 2000; Corney et al. 2006), constituting a likely mechanism responsible for the newly-formed scars due to mass movements in the outer levees shown by Girardclos et al. (2012).

## **Conclusions**

Our multiproxy study based on sediment cores retrieved by manned submersibles and in situ geotechnical measurements has provided new insights into the sedimentary dynamics in the active subaquatic channel of the Rhone delta. Two sedimentary facies have been described in the active canyon: (i) hemipelagic sediments consisting of mm-thick laminated silts, and (ii) turbidites with a fining upwards succession as a result of underflow processes in subaquatic channels. The progressive decrease of sedimentation rate on the northern levee in the down-channel direction, ranging from 2.6 to 1.9 to 0.78 cm/year in the proximal, middle and distal areas, respectively, is in agreement with sedimentation rates in marine deep-water levee sequences, although displaying generally higher values than in the marine realm. Our study emphasizes the high level of activity of sedimentary environments in subaquatic channels, mainly under the effect of underflow processes related to large floods and/or mass movements, and also under the influence of natural and anthropogenic changes in environmental conditions through time.



Ongoing erosional processes control sediment dynamics in the canyon floor while sedimentation dominates in levees. The sedimentological evolution of the canyon towards an increase in flow confinement through time is also apparent in the decrease of the turbidites frequency observed along the proximal canyon walls. Rapid sediment loading, undercutting-induced slope oversteepening, and increase in pore pressure due to high methane concentrations together control the long-term slope instability of the canyon walls. Proximal areas are most prone to mass-movement processes, where coarse turbidites are possible weak layers acting as potential planar surfaces of slide initiation for slope failures. Follow-up research efforts in the Rhone delta canyon will focus on the impact of extreme climatic events on gravity-flow generation and side-wall collapse as well as on the consequences on the meandering evolution of the channel.

**Acknowledgments** This publication is part of the international, interdisciplinary research project ELEMOMO (<http://www.elemo.ch>) to investigate the deep-waters of Lake Geneva using two Russian MIR submarines. We are grateful for the funding and support of this study provided by the Fondation pour l'Etude des Eaux du Léman (FEEL). Complementary funding for travel linked to this article writing was provided by SNF Project Nr. 121666. We thank the Russian MIR crew members ([www.elemo.ch/mir-team](http://www.elemo.ch/mir-team)) for their excellent performance and the SAGRAVE team who provided and operated the platform from which the dives were carried out. We also thank Ulrich Lemmin and Jean-Denis Bourquin for project coordination. The service of Mikhail Kranoperov (Russian Honorary Consulate) as liaison is greatly appreciated. Furthermore, we would specially like to thank Sébastien Sollberger, Andrea Moscariello, Michael Hilbe, Philippe Arpagaus and Stefanie Wirth for their support during the dives and laboratory work.

## References

- Anselmetti FS, Bühler R, Finger D, Girardclos S, Lancini A, Rellstab C, Sturm M (2007) Effects of Alpine hydropower dams on particle transport and lacustrine sedimentation. *Aquat Sci* 69:179–198
- Baas JH, McCaffrey WD, Houghton PDW, Choux C (2005) Coupling between suspended sediment distribution and turbulence structure in a laboratory turbidity current. *J Geophys Res Oceans* 110:C111015
- Bastviken D, Cole J, Pace M, Tranvik L (2004) Methane emissions from lakes: dependence of lake characteristics, two regional assessments, and a global estimate. *Global Biogeochem Cy* 18:GB4009
- Blott SJ, Pye K (2001) Gradistat: a grain size distribution and statistics package for the analysis of unconsolidated sediments. *Earth Surf Proc Land* 26:1237–1248
- Burrus D, Thomas RL, Dominik J, Vernet JP (1989) Recovery and concentration of suspended solids in the upper rhone river by continuous flow centrifugation. *Hydrol Process* 3:65–74
- Canals M, Danovaro R, Heussner S, Lykousis V, Puig P, Trincardi F, Calafat A, Durrieu de Madron X, Palanques A, Sánchez-Vidal A (2009) Cascades in Mediterranean submarine grand canyons. *Oceanography* 22:26–43
- Cantero MI, Cantelli A, Pirmez C, Balachandar S, Mohrig D, Hickson TA, T-h Yeh, Naruse H, Parker G (2012) Emplacement of massive turbidites linked to extinction of turbulence in turbidity currents. *Nature Geosci* 5:42–45
- Coleman JM, Prior DB (1988) Mass wasting on continental margins. *Annu Rev Earth Pl Sc* 16:101–119
- Conway KW, Barrie JV, Picard K, Bornhold BD (2012) Submarine channel evolution: active channels in fjords, British Columbia, Canada. *Geo-Marine Lett* 32(4):301–312
- Corella JP, Amrani A, Sigró J, Morellón M, Rico E, Valero-Garcés B (2011) Recent evolution of Lake Arreo, northern Spain: influences of land use change and climate. *J Paleolimnol* 46:469–485
- Corney RKT, Peakall J, Parsons DR, Elliott L, Amos KJ, Best JL, Keevil GM, Ingham DB (2006) The orientation of helical flow in curved channels. *Sedimentology* 53:249–257
- Dominik J, Loizeau JL, Span D (1992) Radioisotopic evidence of perturbations of recent sedimentary record in lakes: a word of caution for climate studies. *Clim Dynam* 6:145–152
- Driscoll NW, Weissel JK, Goff JA (2000) Potential for large-scale submarine slope failure and tsunami generation along the U.S. mid-Atlantic coast. *Geology* 28:407–410
- Edmonds DA, Slingerland RL (2010) Significant effect of sediment cohesion on delta morphology. *Nat Geosci* 3:105–109
- Finger D, Schmid M, Wüest A (2006) Effects of upstream hydropower operation on riverine particle transport and turbidity in downstream lakes. *Water Resour Res* 42:W08429
- Forel FA (1885) Les ravins sous-lacustres des fleuves glaciaires. *Comptes Rendus de l'Académie des Sciences de Paris*, pp 1–3
- Giovanoli F (1990) Horizontal transport and sedimentation by interflows and turbidity currents in Lake Geneva. In: Tilzer MM, Serruya-Brock C (eds) Large lakes: ecological structure and function. Springer, Berlin, pp 175–195
- Girardclos S, Schmidt OT, Sturm M, Ariztegui D, Pugin A, Anselmetti FS (2007) The 1996 AD delta collapse and large turbidite in Lake Brienz. *Mar Geol* 241:137–154
- Girardclos S, Hilbe M, Corella JP, Loizeau JL, Kremer K, DelSontro T, Arantegui A, Moscariello A, Arlaud F, Akhtman Y, Anselmetti F, Lemmin U (2012) Searching the Rhone delta channel in Lake Geneva since François-Alphonse Forel. *Arch Sci* 65:103–118
- Greene HG, Maher NM, Paull CK (2002) Physiography of the Monterey Bay National Marine Sanctuary and implications about continental margin development. *Mar Geol* 181:55–82
- Hampton MA, Lee HJ, Locat J (1996) Submarine landslides. *Rev Geophys* 34:33–59
- Henrichs SM, Reeburgh WS (1987) Anaerobic mineralization of marine sediment organic matter: rates and the role of anaerobic processes in the oceanic carbon economy. *Geomicrobiol J* 5:191–237
- Houbolt J, Jonker J (1968) Recent sediments in the eastern part of the lake of Geneva (Lac Léman). *Geologie Mijnbouw* 47(2): 131–148
- Hughes Clarke JE, Brucker S, Muggah J, Church I, Cartwright D, Kuus P, Hamilton T, Pratomo D, Eisan B (2012) The Squamish Prodelta, monitoring active landslides and turbidity currents. Canadian Hydrographic Association 2012: The Arctic, old challenges new, Niagara Falls
- Inman DL, Nordstrom CE, Flick RE (1976) Currents in submarine canyons; an air–sea–land interaction. *Annu Rev Fluid Mech* 8:275–310
- Kane IA, McCaffrey WD, Peakall J, Kneller BC (2010) Submarine channel levee shape and sediment waves from physical experiments. *Sediment Geol* 223:75–85
- Komar PD (1973) Continuity of turbidity current flow and systematic variations in deep-sea channel morphology. *Geol Soc Am Bull* 84:3329–3338

- Kremer K, Simpson G, Girardclos S (2012) Giant Lake Geneva tsunami in AD 563. *Nat Geosci* 5:756–757
- Lambert A, Giovanoli F (1988) Records of riverborne turbidity currents and indications of slope failures in the Rhone delta of Lake Geneva. *Limnol Oceanogr* 33:458–468
- Locat J, Lee HJ (2002) Submarine landslides: advances and challenges. *Can Geotech J* 39:193–212
- Loizeau JL (1991) La sédimentation récente dans le delta du Rhône, Léman: processus et évolution. Dissertation, Université de Genève, Genève
- Loizeau JL, Dominik J (2000) Evolution of the upper Rhone river discharge and suspended sediment load during the last 80 years and some implications for Lake Geneva. *Aquat Sci* 62:54–67
- Loizeau JL, Girardclos S, Dominik J (2012) Taux d'accumulation de sédiments récents et bilan de la matière particulaire dans le Léman. *Arch Sci* 65:81–92
- Meybeck M, Blanc P, Moulherac AE, Corvi C (1991) Chemical evidence of water movements in the deepest part of Lake Lemman (Lake Geneva). *Aquat Sci* 53:273–289
- Meyers PA (2003) Applications of organic geochemistry to paleolimnological reconstructions: a summary of examples from the Laurentian great lakes. *Org Geochem* 34:261–289
- Migeon S, Mulder T, Savoye B, Sage F (2006) The Var turbidite system (Ligurian sea, northwestern Mediterranean)—morphology, sediment supply, construction of turbidite levee and sediment waves: implications for hydrocarbon reservoirs. *Geo-Mar Lett* 26:361–371
- Mountjoy JJ, Barnes PM, Pettinga JR (2009) Morphostructure and evolution of submarine canyons across an active margin: Cook Strait sector of the Hikurangi Margin, New Zealand. *Mar Geol* 260:45–68
- Mulder T, Alexander J (2001) The physical character of subaqueous sedimentary density flows and their deposits. *Sedimentology* 48:269–299
- Mulder T, Syvitski JPM, Migeon S, Faugères JC, Savoye B (2003) Marine hyperpycnal flows: initiation, behavior and related deposits. A review. *Mar Petrol Geol* 20:861–882
- Mulder T, Zaragosi S, Garlan T, Mavel J, Cremer M, Sottolichio A, Sénéchal N, Schmidt S (2012) Present deep-submarine canyons activity in the Bay of Biscay (NE Atlantic). *Mar Geol* 295–298:113–127
- Noda A, TuZino T, Furukawa R, Joshima M, Uchida J (2008) Physiographical and sedimentological characteristics of submarine canyons developed upon an active forearc slope: the Kushiro Submarine Canyon, northern Japan. *Geol Soc Am Bull* 120:750–767
- Normark WR, Piper DJW, Hiscott RN (1998) Sea level controls on the textural characteristics and depositional architecture of the Hueneme and associated submarine fan systems, Santa Monica Basin, California. *Sedimentology* 45:53–70
- OFEV, 2009. *Annuaire hydrologique de la Suisse 2008*. Connaissance de l'environnement., in: l'environnement, O.f.d. (ed) Bern; Switzerland
- Peakall J, McCaffrey B, Kneller B (2000) A process model for the evolution, morphology, and architecture of sinuous submarine channels. *J Sediment Res* 70:434–448
- Reeburgh WS (1983) Rates of biogeochemical processes in anoxic sediments. *Annu Rev Earth Pl Sc* 11:269–298
- Reimer PJ, Baillie MGL, Bard E et al (2009) IntCal09 and Marine09 radiocarbon age calibration curves, 0–50,000 years CAL BP. *Radiocarbon* 51:1111–1150
- Reineck HE, Singh IB (1986) Hydrodynamic factors and bedforms in water. In: Reineck HE, Singh IB (eds) *Depositional sedimentary environments: with reference to terrigenous clastics*. Springer, Berlin, Heidelberg, New York, pp 12–21
- Sastre V (2003) Enregistrement sédimentaire de l'évolution de la fréquence des courants de densité originaires du Rhône dans le Léman (France-Suisse) et impact sur la réoxygénation des eaux profondes. Dissertation, University of Geneva, Institut Forel, Geneva
- Sastre V, Loizeau JL, Greinert J, Naudts L, Arpagaus P, Anselmetti F, Wildi W (2010) Morphology and recent history of the Rhone River Delta in Lake Geneva (Switzerland). *Swiss J Geosci* 103:33–42
- Shepard FP (1932) Sediments of the continental shelves. *Geol Soc Am Bull* 43:1017–1039
- Shepard FP, Marshall NF, McLoughlin PA, Sullivan GG (1979) Currents in submarine canyons and other sea valleys. *AAPG Studies in Geology*, Tulsa, Oklahoma
- Siegenthaler C, Sturm M (1991) Slump induced surges and sediment transport in Lake Uri Switzerland. *Verh Int Ver Limnol* 24:955–958
- Skene KI, Piper DJW, Hill PS (2002) Quantitative analysis of variations in depositional sequence thickness from submarine channel levees. *Sedimentology* 49:1411–1430
- Smith DP, Ruiz G, Kvitek R, Iampietro PJ (2005) Semiannual patterns of erosion and deposition in upper Monterey Canyon from serial multibeam bathymetry. *Geol Soc Am Bull* 117:1123–1133
- Smith DP, Kvitek R, Iampietro PJ, Wong K (2007) Twenty-nine months of geomorphic change in upper Monterey Canyon (2002–2005). *Mar Geol* 236:79–94
- Sollberger S, Corella JP, Girardclos S, Randlett ME, Schubert CJ, Senn D, Wehrli B, DelSontro T (2013) Influence of subaquatic canyons on benthic methane fluxes in the Rhone delta (Lake Geneva). *Aquat Sci* (this issue)
- Stark N, Kopf A (2011). Detection and quantification of sediment remobilization processes using a dynamic penetrometer. In: *Proceedings of the OCEANS 2011, Kona, US*
- Stark N, Hanff H, Kopf A (2009a) Nimrod: a tool for rapid geotechnical characterization of surface sediments. *Sea Technol* 50:10–14
- Stark N, Hanff H, Stegmann S, Wilkens R, Kopf A (2009). Geotechnical investigations of sandy seafloors. In: *Proceedings of the MTS/IEEE OCEANS 2009, Biloxi, US*
- Stark N, Hanff H, Svenson C, Ernstsén V, Lefebvre A, Winter C, Kopf A (2011) Coupled penetrometer, MBES and ADCP assessments of tidal variations in surface sediment layer characteristics along active subaqueous dunes, Danish Wadden sea. *Geo-Mar Lett* 31:249–258
- Stark N, Wilkens R, Ernstsén V, Lambers-Huesmann M, Stegmann S, Kopf A (2012) Geotechnical properties of sandy seafloors and the consequences for dynamic penetrometer interpretations: quartz sand versus carbonate sand. *Geotech Geol Eng* 30:1–14
- Strasser M, Stegmann S, Busmann F, Anselmetti FS, Rick B, Kopf A (2007) Quantifying subaqueous slope stability during seismic shaking: lake Lucerne as model for ocean margins. *Mar Geol* 240:77–97
- Sturm M, Matter A (1978) Turbidites and varves in Lake Brienz (Switzerland): deposition of elastic detritus by density currents. *Spec Publ Int Ass Sediment* 2:147–168
- Sultan N, Cochonat P, Canals M, Cattaneo A, Dennielou B, Haflidason H, Laberg JS, Long D, Mienert J, Trincardi F, Urgeles R, Vorren TO, Wilson C (2004) Triggering mechanisms of slope instability processes and sediment failures on continental margins: a geotechnical approach. *Mar Geol* 213:291–321
- Wildi W, Pugin A (1998) Histoire géologique du relief du bassin lémanique. *Arch Sci* 51:5–12

- Wirth SB, Girardclos S, Rellstab C, Anselmetti FS (2011) The sedimentary response to a pioneer geo-engineering project: tracking the Kander River deviation in the sediments of Lake Thun (Switzerland). *Sedimentology* 58:1737–1761
- Wunderlin T, Corella JP, Junier T, Bueche M, Loizeau JL, Girardclos S, Junier P (2013) Endospore-forming bacteria as new proxies to assess impact of eutrophication in Lake Geneva (Switzerland-France). *Aquat Sci* (this issue)
- Xu JP, Noble MA, Rosenfeld LK (2004) In-situ measurements of velocity structure within turbidity currents. *Geophys Res Lett* 31:L09311
- Yoshikawa S, Nemoto K (2010) Seasonal variations of sediment transport to a canyon and coastal erosion along the Shimizu coast, Suruga Bay, Japan. *Mar Geol* 271:165–176